

# New Electro-phases with Tannin Bio-adhesive Produced by Photo cross-linkable Technique

S Abdalla<sup>1,\*</sup>, A. Pizzi<sup>2</sup>, Maryam A. Al-Ghamdi<sup>3</sup>, and Reem Alwafi<sup>1</sup>

<sup>1</sup>Department of Physics, Faculty of Science, King Abdulaziz University Jeddah, P.O. Box 80203, Jeddah 21589, Saudi Arabia

<sup>2</sup>Department Industrial Chemistry ENSTIB-LERMA, University of Lorraine, Epinal, France, Tel: (+33) (0) 329296117, (+33) (0) 329296138

<sup>3</sup>Department of Biochemistry, Faculty of Science, King Abdulaziz University Jeddah, P.O. Box 80203, Jeddah 21589, Saudi Arabia

**Abstract**—rapid cure reactions, low energy demands, solvent free requirements and room temperature use are the advantages of photo polymerization methods compared to thermal techniques. In order to form macromer, tannin polycaprolactone (TPCL) was cross-linked via ultra violet power with 2-isocyanatoethyl methacrylate. Different methods of characterization was carried out estimation of swelling capacity, adhesive capacity (using aminated substrates), surface energy (by contact angle), and attenuated total reflectance Fourier transform infrared. In addition to these experiments, we carried out dynamical mechanical thermal analysis, thermogravimetry and thermogravimetry of TPCL. Thus, one has concluded that the prepared macromer could be transformed into membranes, which were effective as medical adhesive. The degree of cross-linking has been estimated using two different techniques: Swelling of the samples and photo cross-linking of the samples with different periods of irradiation at relatively high UV-power (600mW/cm<sup>2</sup>). Then, we have prepared films of polymer nano-composite (PNC) of poly [vinylidene-fluoride] (PVDF) and bismuth vanadate (BiVO<sub>4</sub>) nanoparticles. The electro-active phases were detected, and the addition of BiVO<sub>4</sub> drastically increases the formation of the  $\alpha$ -phase. Addition of BiVO<sub>4</sub> produces up to 98% of electro-active phases. Robust electrostatic interactions arise between charges at the BiVO<sub>4</sub>-surfaces, and differences in electron affinity between CH<sub>2</sub> and CF<sub>2</sub> groups created dielectric dipoles. The AC-electrical permittivity showed that the dielectric constant of 10%wt- BiVO<sub>4</sub> nanoparticles in PVDF has a value 44  $\epsilon_0$ , which is four times more than the dielectric constant of the as-prepared PVDF films. These data show the importance of these polymers as easy, flexible, and durable energy storage materials.

**Index Terms**—Biopolymers, adhesive, tannin poly caprolacton, isocyanate functional groups.

## 1 INTRODUCTION

As a technique to fill out different injuries, topical skin adhesives guarantee speed, less trauma and less pain. That is why they can do without anesthesia and the problem of stitch removal is eliminated. Bio-adhesives also have the advantage of bringing excellent cosmetic results. In addition, these adhesives are used as delivery frame works that would be further engineered for delayed, localized release of medications, such as pain treatment drugs, antibiotics or chemotherapy. We can use them as mediums for growth factors [1-5] and actual cell lines for healing in tissues such as cartilage that heal poorly [6, 7]. Surgical adhesives control requirements of majority of clinical requirements. Two sides of the tissue must be held together, for as long as necessary before being reduced to suitable bio-products [8]. In addition, an adhesive would make it possible to administer effective treatment in any environment. Fibrin-based adhesives are now the

most commonly used in the medical community [9, 10] along with cyanoacrylates [11, 12]. Several problems are presented by the fibrin based adhesives, e.g. immunogenicity and risk of blood transmission diseases, including the human immunodeficiency virus and the bovine spongiform encephalopathy. On the other hand, to produce formaldehyde, there have been reports of cyanoacrylates degrading in hydrous environment those results in potential cancer or at least sores. Nowadays, there are other options becoming available, with urethane-based adhesives becoming quite promising for this application, among the synthetic materials.

## 2 Experimental

### 2.1 Methods

We have diethyl ether, tannin poly-caprolactone (TPCL) with hydroxyl-end functionalized diol, and 2-isocyanatoethyl methacrylate (IEMA) from Sigma-Aldrich and Merck (Germany). We got human plasma in the fresh frozen state from the KAU-University Hospital. Their frozen state was maintained until we were ready to put them to use. Then, in polypropylene tubes, we collected venous blood (from rabbit) with a 9:1 blood acid citrate dextrose (ACD) solution ratio and made use of them as soon as we collected them; we dented these samples of blood ACD-RB.

- S Abdalla<sup>1</sup> and Reem Al-wafi<sup>1</sup> Department of Physics, Faculty of Science, King Abdulaziz University Jeddah, P.O. Box 80203, Jeddah 21589, Saudi Arabia
- A. Pizzi<sup>2</sup> Department Industrial Chemistry ENSTIB-LERMA, University of Lorraine, Epinal, France, Tel: (+33) (0) 329296117, (+33) (0) 329296138
- Maryam A. Al-Ghamdi<sup>3</sup> Department of Biochemistry, Faculty of Science, King Abdulaziz University Jeddah, P.O. Box 80203, Jeddah 21589, Saudi Arabia

## 2.2 Preparation of samples

Using IEMA and diethyl ether as solvent, we modified hydroxyl end functionalized TPCL diol to synthesize TPCL macromers containing urethane groups. The percentage of isocyanate group (NCO) to hydroxyl groups used was 2:1. The choice of (C<sub>2</sub>H<sub>5</sub>)<sub>2</sub>O as solvent was for its relatively high volatility. Taken account the refluxing of solvent-material and using N<sub>2</sub> as general environmental ambience (without atmospheric air); we performed the reaction by stirring the two materials in a typical special glass- flask. Then at 40°, we put the flask in a H<sub>2</sub>O-bath.

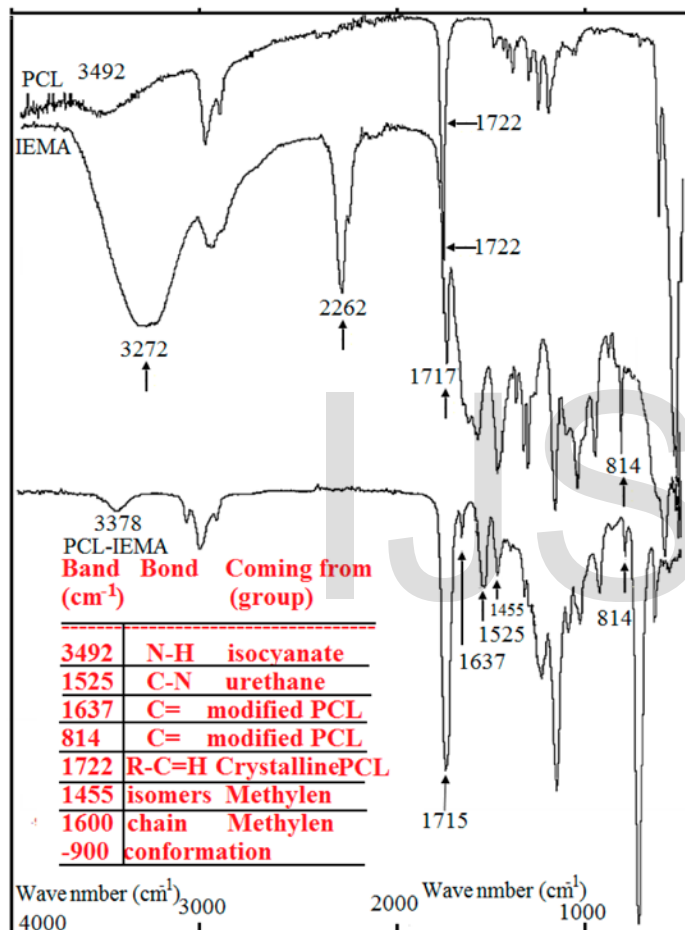


Fig. 1: Before ultraviolet irradiation, the spectrum of attenuated total reflectance Fourier transform infrared spectroscopy due to poly caprolactone (TPCL) adjusted with 2-isocyanatoethyl methacrylate in liquid phase.

C. The formation of urethane groups has been attained using attenuated total reflection infrared spectroscopy (ATR-FTIR) technique. After 24 h of biochemical reaction the totality of isocyanate functional groups with the formula R-N=C=O had completely reacted with the TPCL hydroxyl groups. Using a Buck scientific Spectrometer Magma-IR, we recorded spectra on an average of 128 samples with an excellent resolution of about 4 cm.

## 2.3 Ultra violet irradiation for cross-linked systems

## formation

Using photo cross-linking with ultraviolet technique, we prepared the cross-linked networks; then with a 0.04 molar-solution of the IEMA we added the photo-initiator to the macromer; this was happening while the glass flask was kept in the H<sub>2</sub>O-bath at 60°C. Keeping the mixture with continuous stirring, we waited until all Irgacure 2959 material was dissolved. We removed the resultant solution from the H<sub>2</sub>O-bath and had it irradiated by using a UV lamp (Model UVGL-48, Multiband UV, from Mineral light Lamp) for 60 s. After this period, we obtained a membrane.

## 2.4 Capacity of H<sub>2</sub>O-sorption

Under suitable environmental conditions (e.g. good vacuum conditions), we primarily dried 3 samples compound till they attain unchanged mass (W) at 60°C. We then set these three samples in a suitable vessel with a saturated solution of CuSO<sub>4</sub> · 5H<sub>2</sub>O then recorded their mass at several times to achieve a maximum weight (W<sub>d</sub>); one can estimate the swelling ratio as [13]:

$$\text{SwellingRatio}(\%) = \left( \frac{W_s - W_d}{W_d} \right) \times 100\% \quad (1)$$

## 2.5 Estimation of adhesive capacity: Effect of substrate

To assess the adhering capacity of the macromer, we sandwiched it (as a solution) between two gelatin sheets of dimensions 1.5 × 3 with overlap in 1 cm in which we placed the adhesive. The final dimension of the glued gelatin films was 1.5 × 5 cm in total.

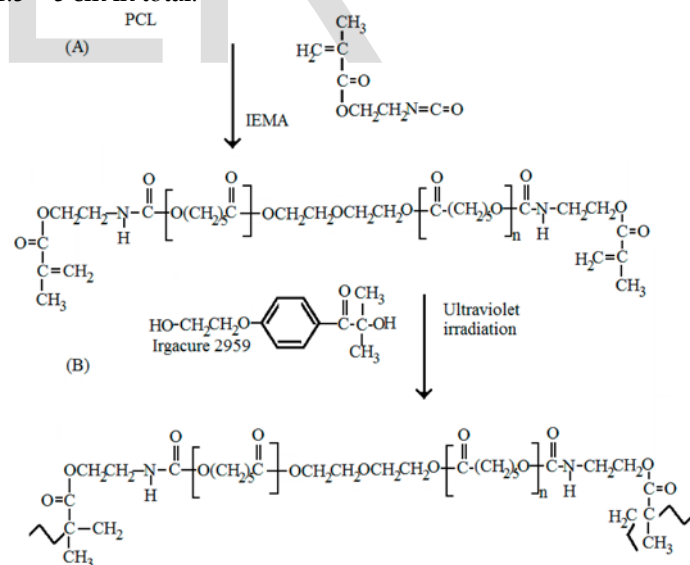


Fig. 2: Sequences of the different reactions, which, lead to the formation of the membrane.

We used ultra violet radiation to treat them using the same conditions as early described by different authors. By this technique, we succeeded to attach the substrates with films. We then subjected the gelatin sheets to the pullout testing where the pulling velocity was 20 mm/ minutes and we established the distance between the probes at 1 cm. We carried

out the assays at room temperature. The apparatus and the software program reported the force as a function of corresponding length. Finally, when gelatin sheets fractured or their separation increased the test got its end. In addition, we performed a negative control test by carrying out the same experimental test with gelatin sheet without any treatment (1.5 × 5 cm). The distance between the probes was 1 cmf and the pulling velocity was established at 20 mm/minutes. We carried out the assays at room temperature. The apparatus and the software program registered the length and force variation. The separation of gelatin sheets or any fracture on them will put off the adhesion tests. We also subjected a gelatin sheet with no treatment (1.5 × 5 cm) to play the role of standard negative reference.

## 2.6 Morphology of samples: SEM-examination

We performed the analyses in a scanning microscope JSM-5310 from Jeol (MA-USA). Different magnifications were taken to get a better view of the surfaces morphology and different cross sections of the membranes. These membranes were placed on carbon stripe, which carefully wrapped with Cu-thin film to permit good vision of cross-linked systems. Just the cross section claimed, we used liquid CO<sub>2</sub> to cool the membranes, which were ready to be fractured.

## 2.7 Plasma degeneration

For a period 6 weeks, we carried out bio-self-elimination studies in human plasma. After well vacuum-drying of membranes, their weights were reported and they were carefully put in glass tube. Then we added 1 mL of plasma to each membrane and incubated the glass tubes at 37° C. After removing three samples from plasma, we used vacuum drying with careful cleaning once more. The weight variations were reported at definite terms: 2 days, 1, 2, 4 and 6 weeks. In order to get clear situation, one of the three samples was retained attached for more scanning electron microscopy test.

## 2.8 Surface properties

The fact that surface energy (SE) is an important parameter affecting polymers adhesion, material wettability and even biocompatibility is widely acknowledged [25]. The measurement of contact angles is deemed the most convenient technique for the determination of the surface free energy of solid samples. This method relies on the determination of the interactions between liquids with well-determined surface tensions and the solid sample of interest. Owens, Wendt, Rabel and Kaelble, maintain that one can divide the interfacial tension in two components: dispersive interactions and polar interactions [27]. Polar interactions bring about Coulomb interactions between permanent dipoles and the ones between permanent and induced dipoles. The interactions caused by time fluctuations of the charge distribution within the molecules are known as dispersive interactions. In the course of this work, we evaluated surface energies of the crosslinked polymer and a gelatin sheet by static contact angle ( $\theta$ ) measurements in an OCA 20 from data physics to make a com-

parison between them and the published data concerning skin and blood. We carried out the necessary tests on the air-facing surfaces of the samples with different solvents such as H<sub>2</sub>O, H-C=O-NH<sub>2</sub>, HO-CH<sub>2</sub>CH<sub>2</sub>2-OH and, HO-CH (CH<sub>3</sub>) CH<sub>2</sub>-OH with the sessile technique. We performed nine measurements on different points to calculate the mean static contact angle  $\theta$  and its standard deviation. We determined the dispersive ( $\gamma_s^D$ ) and polar ( $\gamma_s^P$ ) components of the urethane in addition to the one of the gelatin layers in line with the Owens-Wendt-Rabel and Kaelble relationship [28]. However, before application of photo irradiation the adhesive should be in the liquid form. Therefore, using the Young-Laplace method, we estimated the surface tension of the liquid adhesive with the same apparatus used during surface energy estimation. By applying this technique, we carried out the experimental data by analyzing the situation of an adhesive tinny portion or (hanged-drop) in direct touch with air through time. Using Imai and Nose's gravimetric method [29], we estimated the rate of thrombus formation on 3 specimens of the membrane area. Thus, we, first, used anticoagulated ACD-RB. Then, one prepared this sample wheny putting 1 mL of acid citrate dextrose solution to 9 mL of pure blood. The membranes were immersed in PBS solution at the standard environmental conditions (humidity and temperature-37°C) before performing the tests.

After 48 h of incubation, the PBS was removed and the ACD-RB was placed in contact with the surface of the polymers and with an empty Petri dish acting as a positive control. We initiated blood-clotting tests by adding 0.02 mL of a 0.10 M calcium chloride solution and stopped them after 45 minutes by the addition of 5 mL of water. We fixed the resultant clots with 5 mL of a 36% formaldehyde solution and thendried them with tissue paper before finally weighting them.

We followed the prescriptions of the American Society for Testing and Materials (ASTM, 2000) in performing the haemolysis tests. 7 mL of PBS have been added to 3 specimens of area 21 cm<sup>2</sup> in polypropylene test tubes.

After 3-incubation-days, we replaced the PBS by one mL of ACD-RB of concentration 9mg/mL, here we totally took off PBS and put the ACD-RB instead. Then, we set positive and negative reference samples when putting the equal quantity of ACD-RB to 7 mL of PBS and H<sub>2</sub>O. For half hours, we twice inverted each of the three tubes so it can keep approach with ACD-RB and the material. After completing the incubation process, we centrifuged the samples for half hour at 2000 rpm. Using a spectrophotometer, UV/ visible (Jasco V-550), we estimated the rate of hemoglobin released by haemolysis. This was completed using optical densities (OD) techniques. Then, we calculated the percentage of haemolysis:

$$SwellingRatio(\%) = \left( \frac{W_s - W_d}{W_d} \right) \times 100\% \quad (2)$$

## 2.9 Estimation of adhesive capacity: Effect of substrate

To assess the adhering capacity of the macromer, we sandwiched it (as a solution) between two gelatin sheets of di-

mensions  $1.5 \times 3$  with overlap in 1 cm in which we placed the adhesive. The final dimension of the glued gelatin films was  $1.5 \times 5$  cm in total. We used ultra violet radiation to treat them using the same conditions as early described by different authors [14- 17]. By this technique, we succeeded to attach the substrates with films. We, then, subjected the gelatin sheets to the pullout testing [18, 19] where the pulling velocity was 20 mm/minutes, and we established the distance between the probes at 1 cm. We carried out the assays at room temperature. The apparatus and the software program reported the force as a function of corresponding length. Finally, when gelatin sheets fractured or their separation increased the test got its end. In addition, we performed a negative control test by carrying out the same experimental test with gelatin sheet without any treatment ( $1.5 \times 5$  cm).

The distance between the probes was 1 cmf and the pulling velocity was established at 20 mm/minutes. We carried out the assays at room temperature. The apparatus and the software program registered the length and force variation. The separation of gelatin sheets or any fracture on them will put off the adhesion tests. We also subjected a gelatin sheet with no treatment ( $1.5 \times 5$  cm) to play the role of standard negative reference.

### 3 Results and Discussions

Reaction between polycaprolactone and its hydroxyl derivatives yields a macromere with 2- isocyanatoethyl methacrylate. The creation of urethane groups is the essential feature of this reaction.

In order to be sure that the carbon double bonds terminate the urethanes-compound, a mixture of NCO (2)/ OH (1) groups was used. Illustration on figure 1 shows the presence of bands at  $3378 \text{ cm}^{-1}$  (N-H hydrogen-bonded stretching) and at  $1525 \text{ cm}^{-1}$  (C-N stretching and N-H bending come directly from urethane group).

The functional groups NCO that assess the isocyanate chemically-interact immediately with all the OH- groups in TPCL. This is because we did not observe the presence of the OH groups ( $3492 \text{ cm}^{-1}$ ) in the macromere spectra. Observations of bands at  $1637$  and  $814 \text{ cm}^{-1}$  show that carbon double bonds in the TPCL under test are confirmed. Ultra violet photoinitiator (Irgacure 2959) was used in order to cross-link the macromere as shown in the scheme of the reactions (figure 2). Figure 3 illustrates ATR-FTIR spectrum of the TPCL-IEMA samples. The non-attendance of the carbon double bond is the principal difference shown between the ATR-FTIR carried out before and after the ultra violet irradiation. In addition, we observed that this absence occurs when irradiating with a period at least one minute UV- irradiation.

#### 3.1 Capacity of H<sub>2</sub>O-sorption

Using polymers in different medical applications is a real fact where the swelling capacity of the polymer example, if a polymer placed in vivo, high swelling values will be obtained leading to different side effects as compression of vascular structures. This will lead in turn to some effects as inefficient cicatrization or different types of infections. We obtained rela-

tively low swelling ratios that rise to about 3.21%.

#### 3.2 Estimation of adhesive capacity: Effect of substrate

When sandwiching an adhesive between two gelatin sheets, the binding capacity could be determined with irradiation for 1 minute and subjected to binding strength examination. Here, one can use a sol sample of gelatin as control. The fracture happened at 79 Newton for control gelatin and 70.7 Newton for adhesive gelatin. This means that the urethane was effectively binding the two sheets regardless the glued part. We observed no elongation and the maximum force fractured the control gelatin layer. Control gelatin showed minor mechanical resistance to compressive loads from 0% to 70% strain. At larger strains (70-95%), loads up to  $5 \text{ g/mm}^2$  were recorded, with a mean fracture load of  $4.771.1 \text{ g/mm}^2$ . However, the samples were stiffer at lower strains than control gelatin and significantly stronger with a mean fracture load of  $28.873.9 \text{ g/mm}^2$  at strains ranging from 60% to 85%.

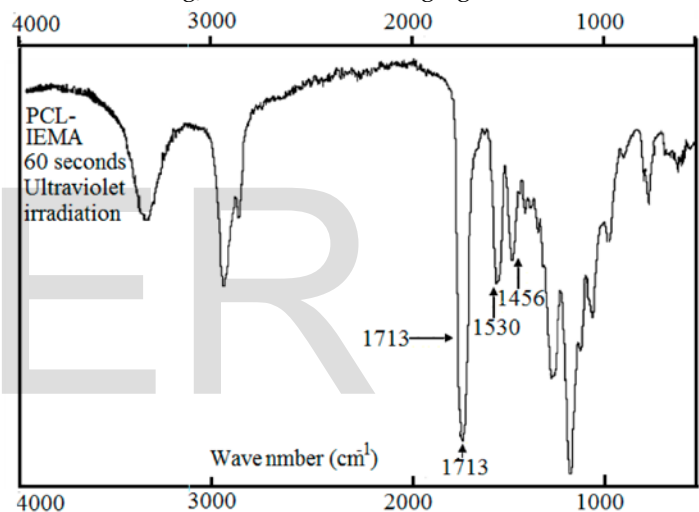


Figure 3: After ultraviolet irradiation, attenuated total reflectance Fourier transform infrared spectroscopy due to the cross-linked polycaprolactone (TPCL) with 2- isocyanatoethyl methacrylate in liquid phase.

One can examine the morphology of the samples with nearly no loss of image tolerance through the analysis. We got different magnification SEM images as shown in figures 4 a- and b. As seen from figure 4, uniform porous structure was detected. This was confirmed when reducing the magnification power which is clearly shown in figure 4-a.

#### 3.3 Morphology of samples: SEM-examination

One can examine the morphology of the samples with nearly no loss of image tolerance through the analysis. We got different magnification SEM images as shown in figures 4 a- and b. As seen from figure 4, uniform porous structure was detected. This was confirmed when reducing the magnification power, which is clearly shown in figure 4-a.

Useful information on the thermal and mechanical properties was obtained using DMTA technique [20].

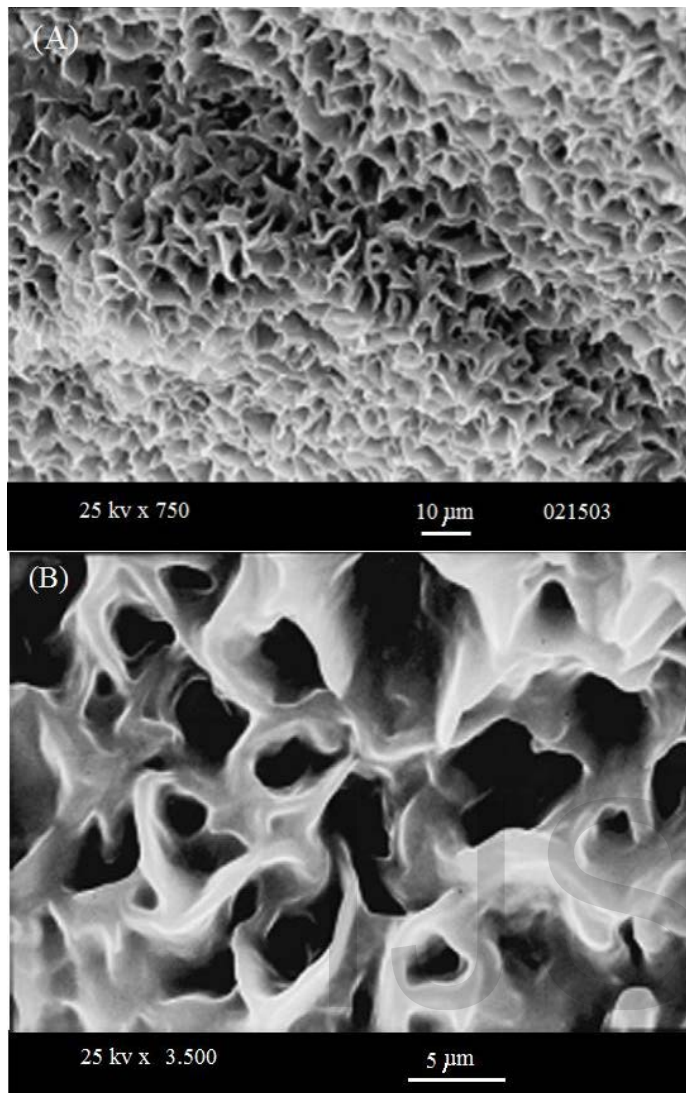


Figure 4: Two different magnifications of the formed-membrane illustrated by scanning electron microscope: (A) magnification 750 x; and (B) magnification 3500x

The gelatin will be deformed if a sinusoidal mechanical load affect on it, on the same time temperature is under controlled and programmable software. Different authors have used the analysis in the constrain layer damping mode with sufficient accuracy [20-23]; we follow this technique with different frequencies as shown in figures 5 and 6. These figures illustrate the unmodified TPCL and the cross-linked mac romere respectively. At 210.7 K (-62.3°C) one can notice the presence of peak which is sensitive to the applied frequency (figure 5).

This peak was attributed to  $T_g$ . Another peak, on the same figure 5 is shown at 262.4K (-10.6°C) but this second is insensitive for frequency and is attributed to the crystallization. The present results are in harmony with previously published data [24- 25]. In addition, a tinny inflexion was detected at 323 K (50 °C) (figure 5) which could be attributed to the phase change of several crystal- line zones of the TPCL. Figure 6 shows a net peak at 233 K (-40 °C) that is sensitive to frequency variations. Thus, this peak is attributed to the

glass transition point  $T_g$ . To estimate the activation energy for alpha relaxation, we used the well known Arrhenius equation:

$$(3) \ln f = \left( \frac{\Delta H}{RT} \right) \quad (3)$$

Here  $f$  is the frequency of analysis,  $R$  is the gas constant,  $\Delta H$  is the activation energy and  $T$  temperature in Kelvin. Noting that the activation energy  $\Delta H$  for TPCL is 42 kJmol<sup>-1</sup> which is by far lower than  $\Delta H$  for the synthesized compound which is 124.4 kJ mol<sup>-1</sup>. Figure 7 illustrates the TGA behavior of the membrane produced by photo-cross-linking and the TPCL-IEMA in liquid conditions.

The reduction of mass-weight loss (WL) of the samples without any UV-irradiation happens in two distinct levels where the former initiates at once without any delay after 303 K (30 °C) which is nearly the melting temperature of the solvent, while the second one happens nearly at 513 K (240 °C) and could correspond to volatilization. The melting temperature of the IEMA is about 484 K (211 °C) but there are no any peak at or around this point which indicates the absence of any unreacted isocyanate.

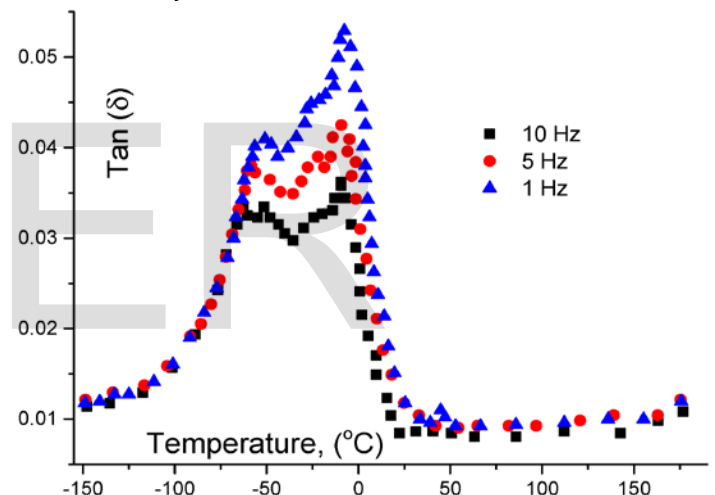


Figure 5: Measurement of the glass transition temperature using dynamic mechanical thermal analysis (DMTA) for poly carpolacton (TPCL). Tangent delta is illustrated as a function of temperature in °C. Measurements were taken at 1, 5, 10 Hz.

The first WL at 303 K (30 °C) is confirmed by the presence of some transitions for the liquid polymer detected by TGA measurements of the membrane (TPCL-IEMA). Also, the WL is better seen in liquid polymer compared to the membrane which shows a second WL at about 599 K (226 °C). These evidences permit us to get a conclusion that compounds with similar thermal stability could be prepared by using the phot-irradiation technique. Nevertheless, at 787 K (514 °C), the polymer is totally degraded and the membrane keep without melting until 873 K (600°C). This gives a net conclusion of increased thermal stability. This is important because when considering our material for biological or/and medical use, it is evidently safe to be used at normal human body temperature 310 K (37 °C) and the compound is thermally stable.

### 3.4 Plasma self-elimination

Figure 8 shows the WL as a function of time and one can see that bio-self-elimination in human plasma follows a logarithmic behavior in this variation which means that WL happens more importantly through the first periods (days) of incubation. We found that 0.6 of the total WL was found after two days of plasma incubation. Moreover, the sample itself lost 0.104 of its initial weight after 6 weeks. This WL occurs initially due to self-elimination due to several bioreactions without any enzymes. In fact, this is a direct result of the sensibility of the C-O-(CH<sub>3</sub>) bond towards addition of H<sub>2</sub>O molecules to substance [26, 27].

### 3.5 Surface properties

The surface energy  $\gamma_S$  of an adhesive is an essential parameter to determine the quality of its function.  $\gamma_S$  should be less than or at least equal to the surface energy of an adherent, which is a necessary condition to fulfill good adhesion [8, 28-30]. The present work aims essentially to estimate how good the adhesive would spread all over bleeding surface (if possible) and in particular over the human leather or over the base of gelatin. For skin, the threshold values of  $\gamma^S$  lies in the range  $38 \text{ mNm}^{-1} < \Delta E_S < 56 \text{ mNm}^{-1}$  depending on skin-humidity and temperature [31]; while the surface tension of blood is about  $55.89 \text{ mNm}^{-1}$  [32].

In addition, the surface tension of the PLC-IEAM was found to be  $33.51 \text{ mNm}^{-1}$ .  $\gamma^S$  of gelatin was found about  $44.24 \text{ mNm}^{-1}$  with a dispersive component ( $\gamma^S$ )<sup>D</sup>  $5.0 \text{ mNm}^{-1}$  and polar component ( $\gamma^S$ )<sup>P</sup>  $39.24 \text{ mNm}^{-1}$ . For cross-linked polymer:  $\gamma^S$   $40.77 \text{ mNm}^{-1}$  ( $\gamma^S$ )<sup>D</sup>  $6.76 \text{ mNm}^{-1}$  and ( $\gamma^S$ )<sup>P</sup>  $34.01 \text{ mNm}^{-1}$ .

One can notice that  $\gamma_S$  for gelatin, skin and blood are stronger than the surface tension of adhesive. Consequently, the adhesive forces will be stronger than the intermolecular forces, which will facilitate the spreading of the liquid adhesive. Using gravimetric techniques, we have estimated the rate of production of thrombus on the surface of the obtained layer. The experimental data show that for the membrane, surface test the rate was 0.03 and it rises up to 0.038 for the blood clots. This means that the cured adhesive has thrombogenic behavior. We did not found an important difference between the two types of thrombus: One formed over control glass and the other formed over the film itself. In fact, this is due to the surface energy of urethanes because proteins are adsorbed immediately and irreversibly at the surface of materials with high surface energy [33, 34].

If one considers that coagulation is formed from consecutive steps; the first one will be the protein adhesion followed by the thrombus formation [35] where the films have thrombogenic behavior. This is of some medical importance because adhesives can be applied in bleeding situations and this material would be developed in order to not only to initiate coagulation but also to stop bleeding.

Figure 10 shows values of haemolysis index of the samples,

which are in direct contact and they did not undergo any chemical-extractions and samples in direct contact incubated in PBS and of the PBS. Under different conditions, the haemolytic index was estimated from contact of the films with Acid-citrate- dextrose blood. The rates of haemolysis for several samples distributing according to American Society for Testing and Materials Standards C756-00 ASTM 2000 as follows: Non- haemolytic with haemolysis rate between 0 up to 2; slightly haemolytic with haemolysis rate between 2 up to 5 and haemolytic with haemolysis rate more than 5. Standard Practices for Assessment of Haemolytic Properties of Materials (USA). Light haemolytic occurs when direct contact takes place. However, the values of haemolysis decrease when extraction with PBS was carried out. These low values are caused by products which were rinsed by PBS and not by the urethane. Although there is no standard universal level of acceptable (or non-acceptable) values of haemolysis, precise estimation of tiny amounts of plasma haemoglobin could be estimated by haemolysis test, which can provide significant screening test. One should take care when using several medical devices that would lead to haemolysis. In addition, we have to be aware about what we will take, as medical interest is greater than the potential risks including that the rates of haemolysis lies in the safe range.

## 4 CONCLUSION

When adjusting hydroxyl-end functionalized TPCL diol with isocyanatoethyl methacrylate, we have prepared macromer with urethane as the effective group in PLC. The prepared macromer is transformed into membranes which was effective as adhesive and it has homogeneous morphology. Experimental data with DMTA and ATR-FTIR have confirmed the creation of material through the given reaction. The obtained macromers have suffered ultra violet irradiations, which leads to membranes formation. The obtained adhesive was effective with homogeneous morphology. The weight loss in the samples correlated with bio-self-elimination reached about 10% after 6 weeks. Indirect contact and extraction with PBS solution eliminated the haemolysis within acceptable and safe ranges.

**ACKNOWLEDGEMENT:** This project was funded by the Deanship of Scientific Research (DSR) at King Abdulaziz University, Jeddah, under grant no. (RG-4-130-37). The authors, therefore, acknowledge with thanks DSR technical and financial support.

**AUTHOR CONTRIBUTIONS:** Authors have contributed equally to this work.

**CONFLICTS OF INTEREST:** The authors declare no conflict of interest.

## REFERENCES:

[1] Feng Chen, Songrui Yu, Bing Liu, Yunzhou Ni, Chunyang

Yu, Yue Su, Xinyuan Zhu, Xiaowei Yu,b, Yongfeng Zhou, and Deyue Yan, An Injectable Enzymatically Crosslinked Carboxymethylated Pullulan/Chondroitin Sulfate Hydrogel for Cartilage Tissue Engineering  
Sci Rep. 2016; 6: 20014. doi: 10.1038/srep20014

[2] Denise Salzig, Jasmin Leber, Katharina Merkewitz, Michaela C. Lange, Natascha Köster, and Peter Czermak, Attachment, Growth, and Detachment of Human Mesenchymal Stem Cells in a Chemically Defined Medium, Stem Cells International Volume 2016 (2016), Article ID 5246584, 10 pages <http://dx.doi.org/10.1155/2016/5246584>

[3] T. Opperman, J. Leber, C. Elseberg, D. Salzig, and P. Czermak, "hMSC production in disposable bioreactors in compliance with cGMP guidelines and PAT," American Pharmaceutical Review, vol. 17, no. 3, pp. 42-47, 2014

[4] Christine V. Benedict, Paul T. Picciano, Bioadhesives for cell and tissue adhesion, USPTO, Patent number US5108923 A 28. Apr. 1992

[5] P. Ferreira, J. F. J. Coelho, J. F. Almeida and M. H. Gil, Photocrosslinkable Polymers for Biomedical Applications, "Biomedical Engineering - Frontiers and Challenges", book edited by Reza Fazel-Rezai, ISBN 978-953-307-309-5, Published: August 1, 2011 under CC BY-NC-SA 3.0 license.

[6] Scognamiglio F, Travan A, Rustighi I, Tarchi P, Palmisano S, Marsich E, Borgogna M, Donati I, de Manzini N, Paoletti S. 2016. Adhesive and sealant interfaces for general surgery applications. J Biomed Mater Res Part B 2016;104B:626-639

[7] Thomas Lally, Multi-Purpose Bio-Material Composition, USPTO, Patent number US20120141596 A1, 25. Sept. 2011

[8] Mohammadreza Mehdizadeh and Jian Yang, Design Strategies and Applications of Tissue Bioadhesives, Macromol Biosci. 2013 Mar; 13(3): 271-288. doi: 10.1002/mabi.201200332

[9] Ebner FM, Paul A, Peters J, Hartmann M. Venous air embolism and intracardiac thrombus after pressurized fibrin glue during liver surgery. Br J Anaesth 2011; 106:180.

[10] Petrie, Edward M, Cyanoacrylate Adhesives in Surgical Applications, Reviews of Adhesion and Adhesives, Number 3, 2014, pp. 253-310(58)

[11] Agarwal A, Jacob S, Kumar DA, Narasimhan S. Handshake technique for glued intrascleral haptic fixation of a posterior chamber intraocular lens. J Cataract Refract Surg. 2013;39:3:317-22.

[12] Manogna RI Vangala, Amrutha Rudraraju, R V Subramanyam, Mounting ground sections of teeth: Cyanoacrylate adhesive versus Canada balsam, J Oral Maxillofac Pathol 2016; 20(1):20-4

[13] Hitesh Chavda, Ishan Modhia, Anant Mehta, Rupal Patel, and Chhagan Patel, Development of Bioadhesive Chitosan Superporous Hydrogel Composite Particles Based Intestinal Drug Delivery System, BioMed Research International Volume 2013 (2013), Article ID 563651, 10 pages, <http://dx.doi.org/10.1155/2013/563651>

[14] Ferreira P, Coelho JF, Gil MH, Development of a new photocrosslinkable biodegradable bioadhesive, Int J Pharm. 2008 Mar 20;352(1-2):172-81. Epub 2007 Dec 11.

[15] Bochyńska AI, Hannink G, Grijpma DW, Buma P. J , Tissue adhesives for meniscus tear repair: an overview of current advances and prospects for future clinical solutions, Mater Sci Mater Med. 2016 May; 27(5):85. Epub 2016 Mar 12.

[16] Annabi N, Yue K, Tamayol A, Khademhosseini A. Elastic sealants for surgical applications, Eur J Pharm Biopharm. 2015 Sep; 95(Pt A):27-39. Epub 2015.

[17] Annabi N, Yue K, Tamayol A, Khademhosseini A. Elastic sealants for surgical applications, Eur J Pharm Biopharm. 2015 Sep; 95(Pt A):27-39. Epub 2015 Jun 12.

[18] Marques D.S. · Santos J.M.C. · Ferreira P. · Correia T.R. · Correia I.J. · Gil M.H. · Baptista C.M.S.G., Photocurable bioadhesive based on lactic acid, Materials Science and Engineering C 58:601-609, 2016, DOI: 10.1016/j.msec.2015.09.009

[19] Correia T.R., Ferreira P. · Vaz R. · Alves P. · Figueiredo M.M. · Correia I.J. Coimbra P., Development of UV cross-linked gelatin coated electrospun poly(caprolactone) fibrous scaffolds for tissue engineering, International Journal of Biological Macromolecules, 2016, DOI: 10.1016/j.ijbio mac.2016.05.045

[20] Ferreira P1, Pereira R, Coelho JF, Silva AF, Gil MH, Modification of the biopolymer castor oil with free isocyanate groups to be applied as bioadhesive, Int. J. Biol. Macromol. 2007 .30;40(2):144-52. Epub 2006.

[21] P. Ferreira, J. F. J. Coelho, R. Pereira, and M. H. Gil, Synthesis and characterization of a poly(ethylene glycol) prepolymer to be applied as a bioadhesive, Journal of Applied Polymer Science 105(2):593 - 601 · July 2007, DOI: 10.1002/app.26206

[22] R.Umamaheswara rao, S.Santhosh Kumar, M.Santhi Kumar, Preparation and Characterization of Polymer Nanocomposites For Damping, International Journal of Engineering Research and Applications (IJERA) ISSN: 2248-9622 www.ijera.com, 2, 4, 2012, pp.1451-1458

[23] Meera Parthasarathy, Swaminathan Sethuraman, Hierarchical Characterization of Biomedical Polymers, Natural and Synthetic Biomedical Polymers, 2014, Pages 33-42

[24] Coelho, J.F.J., Silva, A.M.F.P., Popov, A.V., Percec, V., Abreu, M.V., Gonçalves, P.M.O.F., Gil, M.H., 2006. Single electron transfer-degenerative chain transfer living radical polymerization of N- butyl acrylate catalyzed by Na2S2O4 in water media. J. Polym. Sci., Part A: Polym. Chem. 44, 2809-2825. [25] Santos, K.S.C.R., Coelho, J.F.J., Ferreira, P., Pinto, I., Lorenzetti, S.G., Ferreira, E.I., Higa, O.Z., Gil, M.H., 2006. Synthesis and characterization of membranes obtained by graft copolymerization of 2- hydroxyethyl methacrylate and acrylic acid onto chitosan. Int. J. Pharm. 310, 37-45.

- [26] Yari A, Teimourian S, Amidi F, Bakhtiyari M, Heidari F, Sajedi N, Veijouye SJ, Dodel M, Nobakht M. , The role of biodegradable engineered random polycaprolactone nanofiber scaffolds seeded with nestin-positive hair follicle stem cells for tissue engineering. *Adv Biomed Res.* 2016; 5:22. Epub 2016
- [27] Dehdilani N, Shamsasenjan K, Movassaghpour A, Akbarzadehlaleh P, Amoughli Tabrizi B, Parsa H, Sabagi F. , Improved Survival and Hematopoietic Differentiation of Murine Embryonic Stem Cells on Electrospun Polycaprolactone Nanofiber. *Cell J.* 2016 Winter; 17(4):629-38. Epub 2016.
- [28] M. Schmid and P. Varga, Chapter 4 in: *The Chemical Physics of Solid Surfaces*, Volume 10: Alloy surfaces and surface alloys; ed. by. D. P. Woodruff, Elsevier 2002, ISBN 0-444-51152-0, pp. 118-151
- [29] Jinshan Guo, Wei Wang, Jianqing Hu, Denghui Xie, Ethan Gerhard, Merisa Nisic, Dingying Shan, Guoying Qian, Siyang Zheng, Jian Yang, Synthesis and characterization of antibacterial and antifungal citrate-based mussel-inspired bio-adhesives, *Bio- materials*. Author manuscript; available in PMC 2017 April 1
- [30] Bochyńska AI, Hannink G, Grijpma DW, Buma P. *Journal of Materials Science. Materials in Medicine.* 2016/01/01 00:00; 2785
- [31] Repka MA1, McGinity JW, Physical- mechanical, moisture absorption and bioadhesive properties of hydroxypropylcellulose hotmelt extruded films, *Biomaterials.* 2000 Jul;21(14):1509-17
- [32] HRNČÍŘ E, ROSINA J: Surface tension of blood. *Physiol Res* 46: 319–321, 1997
- [33] T.R. Correia, P. Ferreira, R. Vaz, P. Alves, M.M. Figueiredo, I.J. Correia, P. Coimbra, Development of UV cross-linked gelatin coated electrospun poly(caprolactone) fibrous scaffolds for tissue engineering, *International Journal of Biological Macromolecules*, Available online 13 May 2016, Accepted Manuscript, <http://www.sciencedirect.com/science/article/pii/S0141813016304561>
- [34] Min-Eui Han, Su-Hwan Kim, Hwan D. Kim, Hyun-Gu Yim, Sidi A. Bencherif, Tae-Il Kim, Na- thaniel S. Hwang, Extracellular Matrix-based Cryogels for Cartilage Tissue Engineering, *International Journal of Biological Macromolecules*, Available online 13 May 2016, In Press, Accepted Manuscript, <http://www.sciencedirect.com/science/article/pii/S0141813016304354>
- [35] Thomas Renné, Miroslava Pozgajová, Sabine Grüner, Kai Schuh, Hans-Ulrich Pauer, Peter Burfeind, David Gailani, and Bernhard Nieswandt, Defective thrombus formation in mice lacking coagulation factor XII, *J Exp Med.* 2005 Jul 18; 202(2): 271–281, PMID: PMC2213000, doi: 10.1084/jem.20050664